

Cite this: *Chem. Sci.*, 2018, 9, 8716

All publication charges for this article have been paid for by the Royal Society of Chemistry

Received 13th July 2018

Accepted 17th September 2018

DOI: 10.1039/c8sc03110j

rsc.li/chemical-science

## Base-induced reversible H<sub>2</sub> addition to a single Sn(II) centre†

Roland C. Turnell-Ritson,<sup>a</sup> Joshua S. Sapsford,<sup>a</sup> Robert T. Cooper,<sup>a</sup> Stella S. Lee,<sup>a</sup> Tamás Földes,<sup>b</sup> Patricia A. Hunt,<sup>a</sup> Imre Pápai<sup>a</sup> \* and Andrew E. Ashley<sup>a</sup>

A range of amines catalyse the oxidative addition (OA) of H<sub>2</sub> to [(Me<sub>3</sub>Si)<sub>2</sub>CH]<sub>2</sub>Sn (1), forming [(Me<sub>3</sub>Si)<sub>2</sub>CH]<sub>2</sub>SnH<sub>2</sub> (2). Experimental and computational studies point to 'frustrated Lewis pair' mechanisms in which 1 acts as a Lewis acid and involve unusual late transition states; this is supported by the observation of a kinetic isotope effect (KIE;  $k'_{(H_2)}/k'_{(D_2)} = 1.51 \pm 0.04$ ) for Et<sub>3</sub>N. When DBU is used the energetics of H<sub>2</sub> activation are altered, allowing an equilibrium between 1, 2 and adduct [1·DBU] to be established, thus demonstrating reversible oxidative addition/reductive elimination (RE) of H<sub>2</sub> at a single main group centre.

## Introduction

In the past decade there has been significant interest in transition metal (TM) free systems which activate H<sub>2</sub>.<sup>1</sup> Two main strategies have emerged to facilitate this reactivity: the use of low-valent main group (MG) compounds,<sup>2</sup> and so-called 'frustrated Lewis pairs' (FLPs).<sup>3</sup> In both cases, reactivity arises from simultaneously having access to a high-lying HOMO and low-lying LUMO (Fig. 1). Various low-valent MG compounds containing multiple E–E bonds (E = Al, Si, Ga, Ge, Sn),<sup>4,5</sup> or single-site low-valent centres such as carbenes and heavier tetrylene analogues, have been shown to react with H<sub>2</sub>.<sup>6</sup> The scope of Lewis bases (LBs) and, to a lesser extent, Lewis acids (LAs), which can be used in H<sub>2</sub>-activating FLPs has expanded to include a number of elements from across the periodic table. This is principally due to the readily tuneable steric and electronic profiles of the individual LA and LB sites.<sup>7–9</sup> Many FLP systems display reversible H<sub>2</sub> cleavage, which has facilitated their rapid expansion into the field of catalytic hydrogenation.<sup>10</sup> The same is not true for low-valent MG compounds; examples of reversible H<sub>2</sub> activation are very rare and limited to antiaromatic boracycles,<sup>11</sup> a phosphorus-based singlet biradicaloid,<sup>12</sup> and only one low-valent group 14 compound: a dinuclear Sn(i) distannynes.<sup>13</sup> The design of single-site MG systems which are ergoneutral for H<sub>2</sub> activation requires fine-tuning of thermodynamic (*e.g.* weak E–H bond strengths promoting an accessible formal E<sup>n+2</sup>/E<sup>n</sup> couple) and kinetic factors, both of which are constrained to a mononuclear species, and is hence especially challenging.

The ability of L<sub>2</sub>Sn(II) compounds to undergo OA has been inversely correlated with the size of the singlet–triplet (HOMO–LUMO) gap, which may be diminished through the use of extremely strong  $\sigma$ -donor ligands. Aldridge *et al.* have employed a bis(boryl)tin(II) system to achieve the only example of direct OA of H<sub>2</sub> to a mononuclear Sn(II) centre, irreversibly forming the Sn(IV) dihydride; boryl ligands are even stronger  $\sigma$ -donors than hydride or alkyl ligands, permitting a successful reaction outcome.<sup>6d</sup>

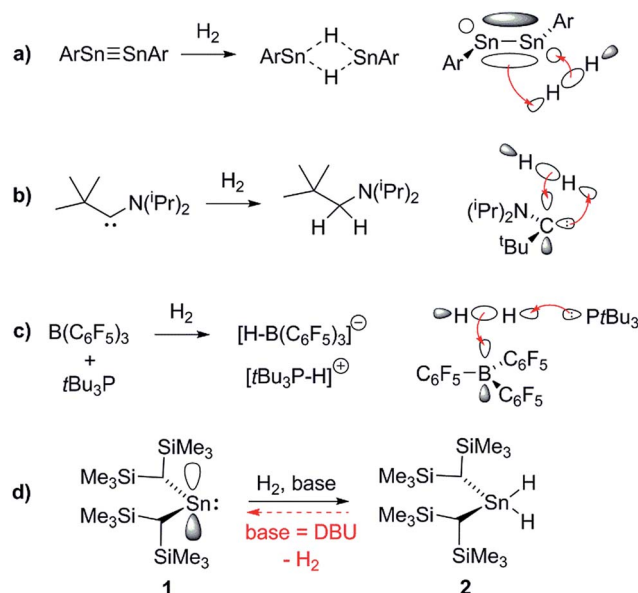


Fig. 1 Representative orbital interactions between H<sub>2</sub> and main group compounds: (a) unsaturated E–E compounds *e.g.* distannynes (Ar = C<sub>6</sub>H<sub>2</sub>-2,6-(C<sub>6</sub>H<sub>3</sub>-2,6-<sup>i</sup>Pr<sub>2</sub>)-4-X; X = H, SiMe<sub>3</sub>, F); for X = H, the reaction is reversible at 80 °C;<sup>5a,13</sup> (b) single site low-valent centres *e.g.* carbenes;<sup>6a</sup> (c) sterically hindered LAs and LBs (FLPs); (d) this work.

<sup>a</sup>Department of Chemistry, Imperial College London, London, SW7 2AZ, UK. E-mail: a.ashley@imperial.ac.uk

<sup>b</sup>Research Center for Natural Sciences, Hungarian Academy of Sciences, Magyar tudósok körútja 2, H-1117 Budapest, Hungary. E-mail: papai.imre@ttk.mta.hu

† Electronic supplementary information (ESI) available: Experimental and computational details. See DOI: 10.1039/c8sc03110j



Conversely, the irreversible base-induced RE of  $H_2$  from organostannanes is well-known.<sup>14</sup> Wesemann and others have studied RE from  $ArSnH_3$  and  $[(Me_3Si)_2CH]SnH_3$  compounds to yield various mononuclear Sn and Sn–Sn bound species ( $Ar$  = terphenyl).<sup>15</sup> Nevertheless, there has yet to be a report of reversible OA and RE occurring on a single Sn(II) scaffold. Lappert's stannylene  $[(Me_3Si)_2CH]_2Sn$  (**1**), which can act as both Lewis acid (LA) and base (LB), is a paradigmatic system for investigating OA to low-valent MG centres, yet to date its reactivity with  $H_2$  has been unexplored.<sup>16</sup> Herein we report the use of FLP methodology to promote formal OA of  $H_2$  to this simple dialkylstannylene. Furthermore we document the first example of reversible  $H_2$  addition to a single-site MG complex, which accesses an FLP *via* reversible dissociation of a classical 1·LB adduct; formation of the latter renders OA of  $H_2$  to **1** energetically less favourable, enabling RE to occur from the Sn(IV) dihydride and reform **1**, which is in equilibrium with 1·LB.<sup>17</sup>

## Results and discussion

**1** is in a rapid solution-phase equilibrium with its dimer  $[1]_2$ , which has been crystallographically characterised and contains a formal Sn=Sn double bond.<sup>18</sup> When a  $d_8$ -toluene solution of  $1/[1]_2$  was placed under an atmosphere of  $H_2$  (4 bar) in a sealed NMR tube, no change was observed in the  $^1H$  NMR spectrum, even after prolonged periods (>48 h), confirming that neither **1** nor  $[1]_2$  can react with  $H_2$  alone. Separately, addition of  $Et_3N$  (20 mol%) to a solution of **1** resulted in no perturbation of their  $^1H$  NMR resonances, suggesting no interaction between the components; *i.e.* the formation of an FLP.<sup>19</sup> Placing this new mixture under  $H_2$  (4 bar, RT) resulted in the solution turning from deep red to colourless over the course of 24 h, with the  $^1H$  NMR spectrum revealing complete consumption of **1** and a new Sn–H triplet resonance at  $\delta = 5.10$  ppm [ $^3J(^1H-^1H) = 2.2$  Hz] with attendant satellites [ $^1J(^{117}Sn-^1H) = 1704$  Hz;  $^1J(^{119}Sn-^1H) = 1784$  Hz], in addition to signals for the  $Si(CH_3)_3$  and methine protons [ $\delta/ppm = 0.17$  (s) and  $-0.42$  (t,  $^3J(^1H-^1H) = 2.2$  Hz), respectively] (see Fig. 2).  $^{119}Sn$  NMR spectroscopy showed only a triplet of triplets at  $-196$  ppm [ $^1J(^{119}Sn-^1H) = 1784$  Hz,  $^2J(^{119}Sn-^1H) = 87$  Hz] which collapsed to a singlet upon  $^1H$  decoupling. Collectively these data correspond to the previously unreported dihydride  $[(Me_3Si)_2CH]_2SnH_2$  (**2**), which was confirmed by comparison with an authentic sample prepared by the reaction of  $LiAlH_4$  and  $[(Me_3Si)_2CH]_2SnCl_2$  (see ESI† for details).

### Isotopic investigation

When  $D_2$  was used in place of  $H_2$ , the methine peak present in the  $^1H$  NMR spectrum of the product mixture resolved as a singlet, while the Sn–H signal was absent and replaced by a Sn–D signal at  $\delta = 5.11$  ppm [ $^1J(^{117}Sn-^2H) = 262$  Hz,  $^1J(^{119}Sn-^2H) = 274$  Hz] in the  $^2H$  NMR spectrum. These results demonstrate the formation of dideuteride **2-D<sub>2</sub>**,<sup>20</sup> and that the Sn-bound protons in **2** must originate from the hydrogen atmosphere.

In order to probe the mechanism further, a  $d_8$ -toluene solution of  $1/[1]_2$  and  $Et_3N$  was reacted with a 1 : 1 mixture of

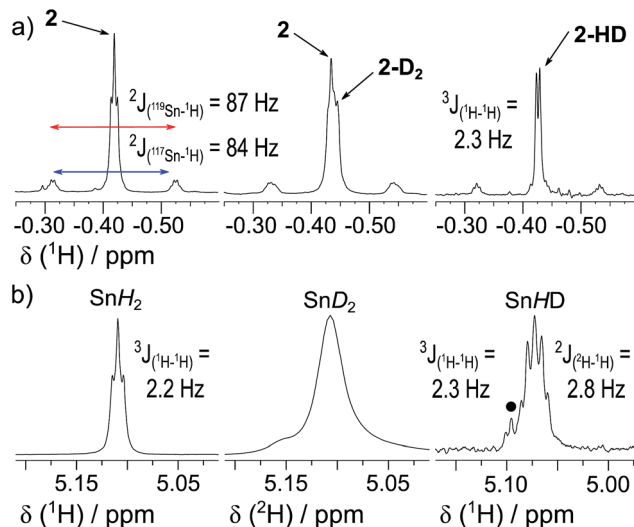


Fig. 2  $^1H/^2H$  NMR spectra from the reaction of **1** and 20 mol%  $Et_3N$ : (a)  $CH(SiMe_3)_2$  region under  $H_2$  (left);  $H_2/D_2$  (1 : 1) (middle); HD (right). (b)  $SnH$  region under  $H_2$  (left);  $H_2/D_2$  (1 : 1) (middle;  $^2H$  NMR); HD (right). ● denotes trace formation of **2** from  $H_2$  in commercial HD gas.

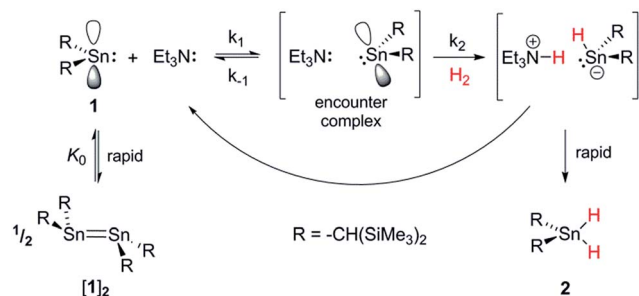
$H_2/D_2$ . The resultant  $^1H$  NMR spectrum was very similar in appearance to that of **2**, with two exceptions: the relative integration of the Sn–H peak did not match that of the methine signal (1.2 : 2; consistent with the faster rate of reaction with  $H_2$  vs.  $D_2$  – *vide infra*), and the C–H resonance was composed of overlapping peaks commensurate with a mixture of **2** and **2-D<sub>2</sub>**. No spectroscopic evidence was seen for the formation of **2-HD**, which was independently and selectively obtained by analogous reaction of  $1/[1]_2$  under an HD atmosphere. These observations provide strong evidence that delivery of both atoms from  $H_2/D_2$ /HD to a single Sn centre occurs either simultaneously, or in a near-concerted fashion.

### Kinetic analysis

By analogy with established FLP systems, and the microscopic reverse of the polar mechanism by which dehydrogenation of  $ArSnH_3$  species is proposed to occur,<sup>15a</sup> we envisaged a reaction mechanism in which **1** and  $Et_3N$  form a weakly associated ‘encounter complex’ which subsequently reacts with  $H_2$  (Scheme 1).<sup>21</sup> Assuming that encounter complex formation is a rapid pre-equilibrium prior to rate-limiting  $H_2$  activation gives the expected rate law: rate =  $k'[1][Et_3N][H_2]$ , where  $k' = (k_1k_2)/k_{-1}$ . Calorimetric studies on  $H_2$  activation by the FLP  $Mes_3P/B(C_6F_5)_3$  ( $Mes = 2,4,6-C_6Me_3H_2$ ) found the rate to be very accurately modelled as a single, termolecular step, which formally gives the same rate law.<sup>22</sup>

To confirm the order of catalytic  $Et_3N$ , the method of time ( $t$ ) scale normalisation was used;<sup>23</sup> normalisation to the scale of  $t \cdot [Et_3N]^x$  resulted in the superposition of all reactant traces only when  $x = 1$ , confirming the rate to be first order with respect to the amine (Fig. 3a). Determination of reaction order with respect to **1** requires its concentration to be known accurately at any given time in a reaction mixture. However, since the





Scheme 1 Proposed reaction mechanism for  $H_2$  heterolysis by **1**, catalysed by  $Et_3N$ .

observed  $^1H$  NMR resonances are a weighted average of the signals from **1** and  $[1]_2$  ( $\Delta G_{293K} = 3.1 \text{ kcal mol}^{-1}$ ), with both species present at significant concentrations under reaction

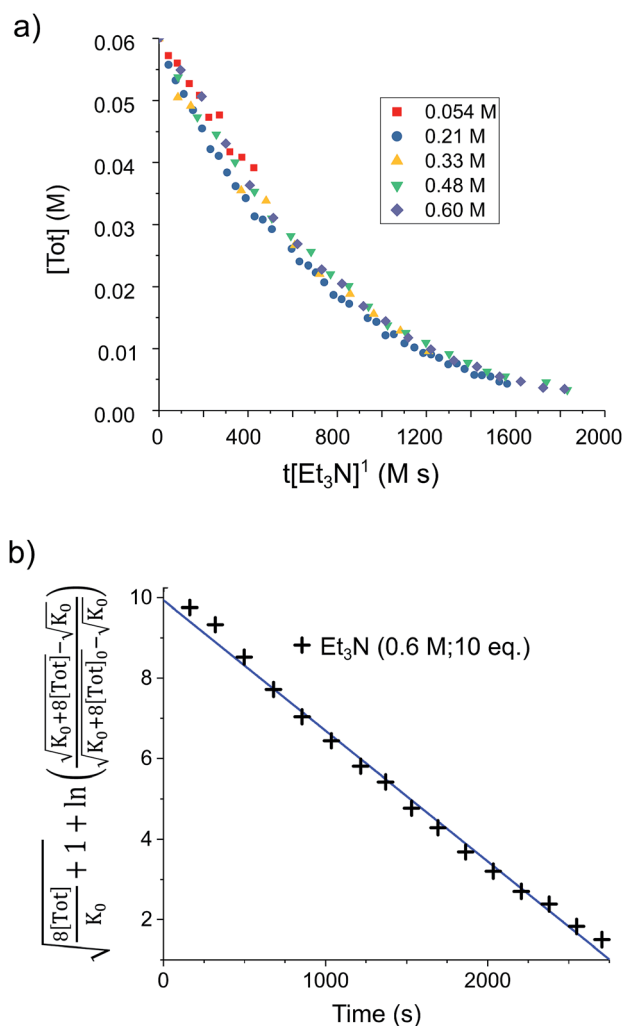


Fig. 3 (a) Solutions of **1** (0.03 mmol) in  $d_8$ -toluene (0.5 mL) under  $H_2$  (4 bar) containing various base concentrations were prepared. When the stannylenes concentration,  $[Tot]$ , is plotted against the normalised timescale  $t \cdot [Et_3N]^1$ , all traces overlap, confirming the order in base to be one. (b) Linearised rate data for a similar solution of **1** (0.03 mmol) in  $d_8$ -toluene (0.5 mL) under  $H_2$  (4 bar) containing  $Et_3N$  (0.6 M; 10 eq.).

conditions, simple observation of the concentration of **1** is not directly possible by  $^1H$  NMR spectroscopy.<sup>18a</sup> The concentration of **1** can, however, be calculated from the total concentration of “ $R_2Sn$ ” species in solution,  $[Tot]$ , present as either monomer or dimer, which are related to the concentrations of **1** and  $[1]_2$  by:

$$[Tot] = [1] + 2[1]_2 \quad (1)$$

The dimerisation equilibrium of **1** can be expressed as:

$$K_0 = \frac{[1]^2}{[1]_2} \quad (2)$$

Combining eqn (1) and (2) and solving for  $[1]$  yields:

$$[1] = \frac{1}{4} \left( \sqrt{K_0} \sqrt{8[Tot] + K_0} - K_0 \right) \quad (3)$$

Inserting eqn (3) into the expected rate law (*vide supra*) gives:

$$-\frac{d[Tot]}{dt} = \frac{k^*}{4} \left( \sqrt{K_0} \sqrt{8[Tot] + K_0} - K_0 \right) \quad (4)$$

where, if the amount of  $H_2$  is sufficiently high that its concentration remains approximately constant:

$$k^* = \frac{k_1 k_2}{k_{-1}} [B] [H_2] \quad (5)$$

Rearrangement and integration by substitution of eqn (4) (see ESI†) gives:

$$\sqrt{\frac{8[Tot]}{K_0}} + 1 + \ln \left( \frac{\sqrt{K_0 + 8[Tot]} - \sqrt{K_0}}{\sqrt{K_0 + 8[Tot]_0} - \sqrt{K_0}} \right) - \sqrt{\frac{8[Tot]_0}{K_0}} + 1 = -k^* t \quad (6)$$

Therefore, plotting the variable portion of the LHS of this expression against  $t$  gives a straight line of gradient  $-k^*$ , confirming the proposed first-order dependence on **1** (Fig. 3b).

Using the known value of  $[H_2]$  in toluene at 4 bar (293 K)<sup>24</sup> provides a value of  $k'_{(Et_3N)} = 0.47 \pm 0.03 \text{ M}^{-1} \text{ s}^{-1}$ .<sup>25</sup> As well as  $Et_3N$ , 2-*tert*-butyl-1,1,3,3-tetramethylguanidine (Barton's base, TBTMG) and 1,2,2,6,6-pentamethylpiperidine (PMP), were also found to form FLPs with **1**/ $[1]_2$ , with corresponding rates of  $H_2$  cleavage:  $k'_{(TBTMG)} = 5.0 \pm 0.3 \text{ M}^{-1} \text{ s}^{-1}$ ,  $k'_{(PMP)} = 0.0266 \pm 0.0018 \text{ M}^{-1} \text{ s}^{-1}$ .<sup>26</sup> Despite the similar basicity to  $Et_3N$ , the bulkier Hünig's base ( $iPr_2EtN$ ;  $pK_{a(MeCN)}$ : 18.0)<sup>27</sup> was ineffective for  $H_2$  heterolysis, as was the weaker base 2,4,6-collidine ( $pK_{a(MeCN)}$ : 14.98).<sup>28</sup> Clearly  $H_2$  activation requires that the LB be sufficiently basic and not too sterically encumbered, in line with observations of other FLP systems.<sup>29</sup>

A kinetic analysis of the isotopic systems permitted quantification of the KIE:  $k'_{(H_2)}/k'_{(D_2)} = 1.51 \pm 0.04$  when  $Et_3N$  was used as the base. In addition, the acceleration in rate from a more polar solvent could also be quantified:  $k'_{(THF)}/k'_{(toluene)} = 1.97 \pm 0.04$  (when  $Et_3N$  was used).



## Coordinating bases

When the less sterically bulky 1,8-diazabicyclo[5.4.0]undec-7-ene (DBU) is used, an interaction with **1** can be clearly seen in the  $^{13}\text{C}\{^1\text{H}\}$  NMR spectrum: upon gradual addition of DBU to **1**/[**1**]<sub>2</sub>, the methine resonance undergoes a substantial upfield shift, reaching a limiting value of  $\delta = 18.5$  ppm (10-fold excess of DBU). Using the established  $^{13}\text{C}$  NMR chemical shift values for **1** and [**1**]<sub>2</sub> (60.0 ppm and 28.7 ppm, respectively),<sup>18a</sup> this is consistent with a fast equilibrium between **1**·DBU, **1** and [**1**]<sub>2</sub> (Scheme 2; see ESI† for full details). A value of  $\Delta G = -3.7 \pm 0.2$  kcal mol<sup>-1</sup> for the formation of **1**·DBU from [**1**]<sub>2</sub> was obtained from a van't Hoff analysis of variable temperature UV-Vis spectra.

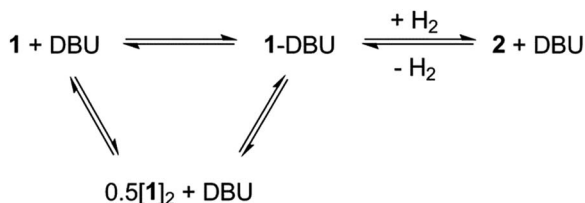
While the reaction of **1**/DBU mixtures (containing 0.1–10 equivalents of DBU) with H<sub>2</sub> proceed rapidly, they do not reach completion, indicative of a reversible process (see Fig. S7 in ESI†).

The reversibility can be explicitly demonstrated by the (CH<sub>3</sub>)<sub>3</sub>Si region of the  $^1\text{H}$  NMR spectrum, whereby addition of DBU to a solution of **2** led to the appearance of a signal corresponding to the dehydrogenated mixture **1**·DBU  $\leftrightarrow$  **1**  $\leftrightarrow$  [**1**]<sub>2</sub>; this increased in intensity at the expense of the (CH<sub>3</sub>)<sub>3</sub>Si peak of **2** (Fig. 4a–c). No H<sub>2</sub> is observed in the  $^1\text{H}$  NMR spectrum as the solution was degassed multiple times in order to accelerate the reaction – however, the very small amount of H<sub>2</sub> generated (approx. 0.3 bar) would likely hamper detection. Furthermore, the methine resonance of the **1**·DBU  $\leftrightarrow$  **1**  $\leftrightarrow$  [**1**]<sub>2</sub> mixture is subject to a significant upfield shift compared to [**1**]/[**1**]<sub>2</sub> (dependent upon the DBU concentration), and so is obscured beneath the relatively intense (CH<sub>3</sub>)<sub>3</sub>Si region. Upon charging this reaction with H<sub>2</sub>, restoration of **2** was rapidly observed (Fig. 4d). For the equilibrium involving H<sub>2</sub> (Scheme 2), an equilibrium constant,  $K_{\text{eq}} = 164 \pm 5$ , in favour of **2** can be calculated from the relative intensities of the (CH<sub>3</sub>)<sub>3</sub>Si resonances, providing  $\Delta G = -3.0$  kcal mol<sup>-1</sup> (1 bar H<sub>2</sub>).

Using the similarly unhindered but less basic 4-(dimethylamino)pyridine (DMAP) also gave an adduct **1**·DMAP, but no reaction with H<sub>2</sub> at room temperature. However, heating a solution of **1** with excess DMAP (4 bar H<sub>2</sub>, 2 h, 100 °C) yielded **2** in 31% conversion.

## Computational investigation

To gain further insight into the mechanism of H<sub>2</sub> activation, DFT calculations were performed for various **1**/LB pairs;<sup>31</sup> the computed reaction profiles for both the Et<sub>3</sub>N- and DBU-



Scheme 2 Equilibrium between product **2** + DBU and the dehydrogenated mixture **1**·DBU  $\leftrightarrow$  **1**  $\leftrightarrow$  [**1**]<sub>2</sub>.

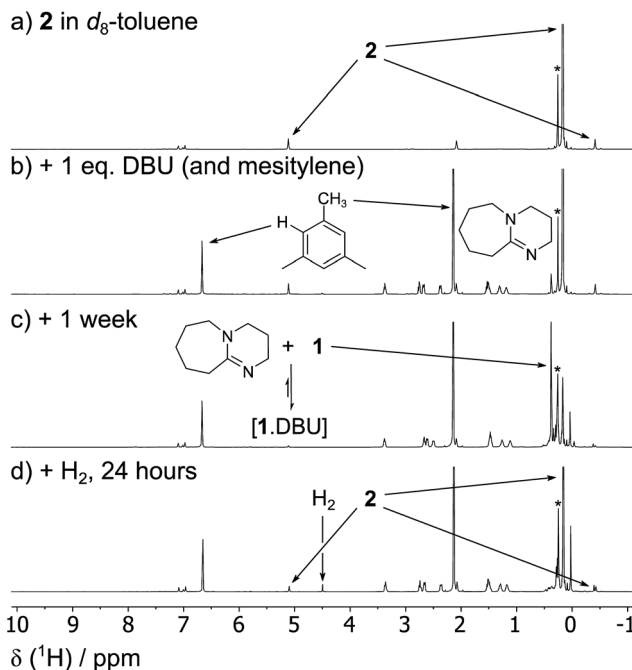


Fig. 4 The reversibility of the reaction between **1**/[**1**]<sub>2</sub>, DBU and H<sub>2</sub> can be shown explicitly by a series of  $^1\text{H}$  NMR spectra depicting: (a) a solution of **2** (0.03 mmol) in  $d_8$ -toluene (0.5 mL) (b) the same solution with added DBU (0.03 mmol, 1 equivalent) and mesitylene (2%) as an internal standard; (c) after degassing three times over the course of one week, showing the formation of **1**·DBU  $\leftrightarrow$  **1**  $\leftrightarrow$  [**1**]<sub>2</sub>; (d) reformation of **2** after the addition of H<sub>2</sub> (4 bar). \*Small amount of silicone grease from the independent synthesis of **2**.

mediated reactions are depicted in Fig. 5. When LB = Et<sub>3</sub>N, the reaction was found to proceed *via* initial H<sub>2</sub> heterolysis leading to a tight ion pair intermediate [**1**H]<sup>−</sup>[Et<sub>3</sub>NH]<sup>+</sup> (**int**<sub>1</sub>). Facile rearrangement to **int**<sub>2</sub> and subsequent delivery of the H<sup>+</sup> to the lone pair on the [**1**H]<sup>−</sup> moiety furnishes **2** (Fig. 6a); a very similar mechanism was found when LB = DBU. In support of this polar mechanism, the rate using Et<sub>3</sub>N as the LB was found to be faster in THF ( $k'_{\text{THF}}/k'_{\text{toluene}} = 1.97 \pm 0.04$ ). The low

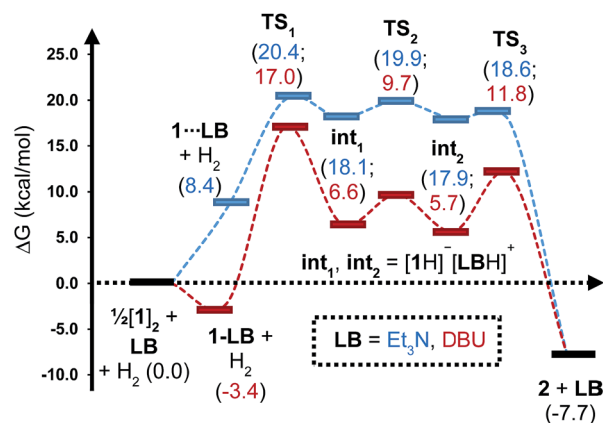


Fig. 5 Computed free energy profile for Et<sub>3</sub>N- and DBU-assisted H<sub>2</sub> activation with **1**. Relative free energies (in kcal mol<sup>-1</sup>) are with respect to 0.5·[**1**]<sub>2</sub> + LB + H<sub>2</sub>.



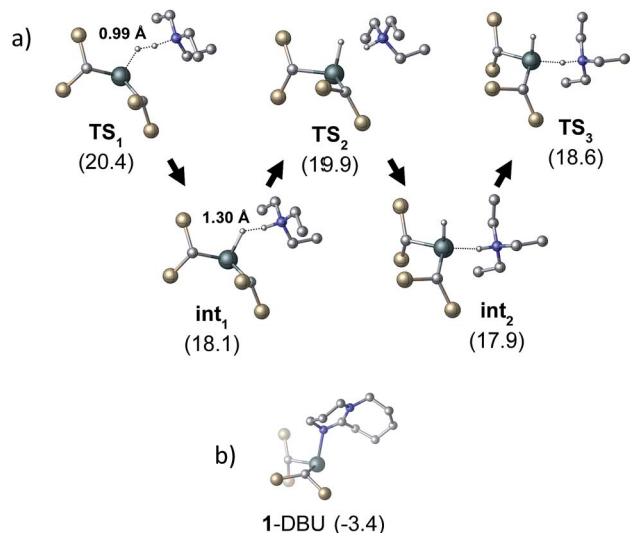


Fig. 6 (a) Structural representations of the computed transition states for the heterolysis of  $\text{H}_2$  by **1** and  $\text{Et}_3\text{N}$ . H–H distances are given for  $\text{TS}_1$  and  $\text{int}_1$ . (b) The computed adduct formed between **1** and DBU. All energies (in  $\text{kcal mol}^{-1}$ ) are relative to  $0.5 \cdot [\text{1}]_2 + \text{LB} + \text{H}_2$ . Si–CH<sub>3</sub> and C–H groups omitted for clarity.

barriers to rearrangement of the intermediates also offer an explanation as to why H/D exchange is not observed upon reaction with an  $\text{H}_2/\text{D}_2$  mixture or HD: collapse of the ion pairs is likely much faster than solvent cage escape.

Although the located transition states (TSs) are energetically close-lying, the overall reaction barrier appears to be determined by the  $\text{H}_2$  splitting step, which is in line with kinetic measurements. Free energy data computed for the  $\text{H}_2$  splitting step for reactions with different bases are compiled in Table 1 alongside other properties. For  $\text{Et}_3\text{N}$ , TBTMG and PMP, no favourable adduct formation was found with **1**, and the  $\Delta G^\ddagger$  values follow the order TBTMG <  $\text{Et}_3\text{N}$  < PMP, which is consistent with experimental reaction rates. For the coordinating bases DBU (Fig. 6b) and DMAP, adducts favourable relative to free  $[\text{1}]_2$  and base were computationally determined. This reduces the absolute value of  $\Delta G_{\text{reaction}}$  such that an

Table 1 Computational and  $\text{pK}_a$  data for reactions of a series of bases with **1** and  $\text{H}_2$ <sup>a</sup>

Property	$\text{Et}_3\text{N}$	TBTMG	PMP	DBU	DMAP
$\text{1} \cdot \text{LB}^a$	—	—	—	−3.4	−3.6
$\text{TS}_1^a$	20.4	18.3	21.4	17.0	20.1
$\text{int}_1^a$	18.1	5.4	16.1	6.6	16.8
$\Delta G^\ddagger^a$	20.4	18.3	21.4	20.4	23.7
$\Delta G_{\text{reaction}}^a$	−7.7	−7.7	−7.7	−4.3	−4.1
$\text{PA}^{a,b}$	−270.1	−286.0	−272.7	−283.5	−272.2
$\text{pK}_a^c$	18.8	23.6	18.7	24.3	18.0
$d(\text{H-H})^{d,e}$	0.99	0.87	0.96	0.88	0.99

<sup>a</sup> Free energy data relative to  $0.5 \cdot [\text{1}]_2 + \text{base} + \text{H}_2$  ( $\text{kcal mol}^{-1}$ );  $\Delta G^\ddagger$  is activation free energy. <sup>b</sup> Proton affinity is defined as the free energy of  $\text{base} + \text{H}^+ \rightarrow \text{baseH}^+$ . <sup>c</sup> Measured in MeCN.<sup>30</sup> <sup>d</sup> H–H distance in  $\text{TS}_1$  (0.76 Å in free  $\text{H}_2$ ).

equilibrium is experimentally observed in the case of DBU. For DMAP, the activation barrier is found to be much higher, paralleling results seen by experiment where elevated temperatures are required to obtain product **2**.

The energies of all intermediates  $\text{int}_1$  are computed to be well above the reference state, which follows from the weak Lewis acidity of **1**. The stabilities of  $\text{int}_1$  species correlate very well with the general trend in PA and  $\text{pK}_a$ , but this is not strictly true for the TSs, where steric factors are more important. Unstable  $\text{int}_1$  intermediates imply late TSs for the  $\text{H}_2$  activation step, which is shown by significantly elongated H–H distances in the TS structures. The experimentally observed KIE ( $1.51 \pm 0.04$ ) supports this finding, which is commensurate with rate-limiting  $\text{H}_2/\text{D}_2$  activation involving considerable H–H/D–D bond breaking.<sup>32</sup>

## Conclusions

In conclusion, we have demonstrated the ability of FLP-mediated reactivity to enable the formal oxidative addition of  $\text{H}_2$  to an otherwise inert MG centre, and in doing so have also observed the first example of reversible  $\text{H}_2$  addition to a single-site MG complex. We have utilised experimental and computational means to comprehensively explore the mechanism of this transformation and found that  $\text{H}_2$  activation in this system differs from those based on more typical FLPs, due to the high-energy nature of the immediate  $\text{H}_2$  splitting products, resulting in rare examples of late TSs. The development of methods to harness this FLP-promoted OA/RE  $\text{H}_2$  reactivity for hydrogenation catalysis is currently underway.

## Conflicts of interest

There are no conflicts to declare.

## Acknowledgements

We wish to thank the EPSRC (J. S. S. and R. T. C; EP/N026004) and an Imperial College President's PhD Scholarship (R. C. T.-R.) for PhD funding and the Royal Society for a University Research Fellowship (AEA; UF/160395). This work was also supported by NKFIH (K-115660).

## Notes and references

- (a) A. L. Kenward and W. E. Piers, *Angew. Chem., Int. Ed.*, 2008, **47**, 38; (b) P. P. Power, *Nature*, 2010, **463**, 171; (c) D. W. Stephan and G. Erker, *Angew. Chem., Int. Ed.*, 2010, **49**, 46; (d) D. Martin, M. Soleilhavoup and G. Bertrand, *Chem. Sci.*, 2011, **2**, 389.
- (a) P. P. Power, *Acc. Chem. Res.*, 2011, **44**, 627; (b) T. Chu and G. I. Nikonov, *Chem. Rev.*, 2018, **118**, 3608.
- (a) F.-G. Fontaine and D. W. Stephan, *Philos. Trans. R. Soc., A*, 2017, **375**, 2101; (b) D. W. Stephan and G. Erker, *Angew. Chem., Int. Ed.*, 2015, **54**, 6400; (c) D. W. Stephan, *Science*, 2016, **354**, 1248.



- 4 First example of a MG compound to activate H<sub>2</sub> under facile conditions: G. H. Spikes, J. C. Fettinger and P. P. Power, *J. Am. Chem. Soc.*, 2005, **127**, 12232.
- 5 (a) Y. Peng, M. Brynda, B. D. Ellis, J. C. Fettinger, E. Rivard and P. P. Power, *Chem. Commun.*, 2008, **45**, 6042; (b) Z. Zhu, X. Wang, Y. Peng, H. Lei, J. C. Fettinger, E. Rivard and P. P. Power, *Angew. Chem., Int. Ed.*, 2009, **48**, 2031; (c) K. Nagata, T. Murosaki, T. Agou, T. Sasamori, T. Matsuo and N. Tokitoh, *Angew. Chem., Int. Ed.*, 2016, **55**, 12877; (d) A. Rit, J. Campos, H. Niu and S. Aldridge, *Nat. Chem.*, 2016, **8**, 1022; (e) T. Kosai and T. Iwamoto, *J. Am. Chem. Soc.*, 2017, **139**, 18146; (f) D. Wendel, T. Szilvási, C. Jandl, S. Inoue and B. Rieger, *J. Am. Chem. Soc.*, 2017, **139**, 9156.
- 6 (a) G. D. Frey, V. Lavallo, B. Donnadieu, W. W. Schoeller and G. Bertrand, *Science*, 2007, **316**, 439; (b) Y. Peng, J. D. Guo, B. D. Ellis, Z. Zhu, J. C. Fettinger, S. Nagase and P. P. Power, *J. Am. Chem. Soc.*, 2009, **131**, 16272; (c) A. V. Protchenko, K. H. Birj Kumar, D. Dange, A. D. Schwarz, D. Vidovic, C. Jones, N. Kaltsoyannis, P. Mountford and S. Aldridge, *J. Am. Chem. Soc.*, 2012, **134**, 6500; (d) A. V. Protchenko, J. I. Bates, L. M. A. Saleh, M. P. Blake, A. D. Schwarz, E. L. Kolychev, A. L. Thompson, C. Jones, P. Mountford and S. Aldridge, *J. Am. Chem. Soc.*, 2016, **138**, 4555; (e) D. Wendel, A. Porzelt, F. A. D. Herz, D. Sarkar, C. Jandl, S. Inoue and B. Rieger, *J. Am. Chem. Soc.*, 2017, **139**, 8134.
- 7 First example of FLP-mediated H<sub>2</sub> heterolysis: G. C. Welch, R. R. San Juan, J. D. Masuda and D. W. Stephan, *Science*, 2006, **314**, 1124.
- 8 For a review detailing the scope of MG LAs in FLP chemistry see: S. A. Weicker and D. W. Stephan, *Bull. Chem. Soc. Jpn.*, 2015, **88**, 1003.
- 9 For FLP H<sub>2</sub> activation mediated by a Sn LA see: D. J. Scott, N. A. Phillips, J. S. Sapsford, A. C. Deacy, M. J. Fuchter and A. E. Ashley, *Angew. Chem., Int. Ed.*, 2016, **55**, 14738.
- 10 (a) D. W. Stephan, S. Greenberg, T. W. Graham, P. Chase, J. J. Hastie, S. J. Geier, J. M. Farrell, C. C. Brown, Z. M. Heiden, G. C. Welch and M. Ullrich, *Inorg. Chem.*, 2011, **50**, 12338; (b) D. J. Scott, M. J. Fuchter and A. E. Ashley, *Chem. Soc. Rev.*, 2017, **46**, 5689.
- 11 (a) A. Y. Houghton, V. A. Karttunen, W. E. Piers and H. M. Tuononen, *Chem. Commun.*, 2014, **50**, 1295; (b) E. von Grotthuss, M. Diefenbach, M. Bolte, H. W. Lerner, M. C. Holthausen and M. Wagner, *Angew. Chem., Int. Ed.*, 2016, **55**, 14067.
- 12 A. Hinz, A. Schulz and A. Villingner, *Angew. Chem., Int. Ed.*, 2016, **55**, 12214.
- 13 S. Wang, T. J. Sherbow, L. A. Berben and P. P. Power, *J. Am. Chem. Soc.*, 2018, **140**, 590.
- 14 (a) H. G. Kuivila, A. K. Sawyer and A. G. Armour, *J. Org. Chem.*, 1961, **26**, 1426; (b) W. P. Neumann and K. König, *Justus Liebigs Ann. Chem.*, 1964, **677**, 1; (c) W. P. Neumann and K. König, *Justus Liebigs Ann. Chem.*, 1964, **677**, 12.
- 15 (a) C. P. Sindlinger, A. Stasch, H. F. Bettinger and L. Wesemann, *Chem. Sci.*, 2015, **6**, 4737; (b) J.-J. Maudrich, C. P. Sindlinger, F. S. W. Aicher, K. Eichele, H. Schubert and L. Wesemann, *Chem.-Eur. J.*, 2017, **23**, 2192; (c) C. P. Sindlinger and L. Wesemann, *Chem. Sci.*, 2014, **5**, 2739; (d) C. P. Sindlinger, W. Grahneis, F. S. W. Aicher and L. Wesemann, *Chem.-Eur. J.*, 2016, **22**, 7554; (e) J. Klösener, M. Wiesemann, M. Niemann, B. Neumann, H.-G. Stammer and B. Hoge, *Chem.-Eur. J.*, 2018, **24**, 4412.
- 16 (a) P. J. Davidson, D. H. Harris and M. F. Lappert, *J. Chem. Soc., Dalton Trans.*, 1976, **21**, 2268; (b) The OA of reactive heteropolar and homopolar bonds (e.g. alkyl halides, Br<sub>2</sub>) has been documented: M. J. S. Gynane, M. F. Lappert, S. J. Miles, A. J. Carty and N. J. Taylor, *J. Chem. Soc., Dalton Trans.*, 1977, 2009; (c) J. D. Cotton, P. J. Davidson and M. F. Lappert, *J. Chem. Soc., Dalton Trans.*, 1976, 2275.
- 17 A cyclic dialkylsilylene, Z. Dong, Z. Li, X. Liu, C. Yan, N. Wei, M. Kira and T. Müller, *Chem.-Asian J.*, 2017, **12**, 1204, has been shown to act as either a LA or LB to activate H<sub>2</sub> in partnership with other LBs/LAs, forming . However, this reaction was irreversible; see . In part, the different reversible behaviour of R<sub>2</sub>Sn in this work is likely a consequence of the weaker Sn-H vs. Si-H bond strength, which renders the thermodynamics of RE more favourable (see ref. 6d).
- 18 (a) K. W. Zilm, G. A. Lawless, R. M. Merrill, J. M. Millar and G. G. Webb, *J. Am. Chem. Soc.*, 1987, **109**, 7236; (b) R. Sedlak, O. A. Stasyuk, C. Fonseca Guerra, J. Řezáč, A. Růžicka and P. Hobza, *J. Chem. Theory Comput.*, 2016, **12**, 1696.
- 19 The <sup>119</sup>Sn NMR resonance for **1** can only be observed in dilute samples and at high temperature (*T* > 345 K), while that for [**1**]<sub>2</sub> can only be resolved at *T* < 225 K. At intermediate temperatures no signal is observable, which prevents an assessment of interaction between the two tin species and Et<sub>3</sub>N using <sup>119</sup>Sn NMR under relevant reaction conditions. See ref. 18a.
- 20 A 1 : 2 : 3 : 2 : 1 multiplet was also observed in the <sup>119</sup>Sn NMR spectrum from <sup>1</sup>J(<sup>119</sup>Sn-<sup>2</sup>H) coupling. See Fig. S3 in ESI†
- 21 (a) L. Rocchigiani, G. Ciancaleoni, C. Zuccaccia and A. MacChioni, *J. Am. Chem. Soc.*, 2014, **136**, 112; (b) T. A. Rokob, A. Hamza, A. Stirling, T. Soós and I. Pápai, *Angew. Chem., Int. Ed.*, 2008, **47**, 2435.
- 22 A. Y. Houghton and T. Autrey, *J. Phys. Chem. A*, 2017, **121**, 8785.
- 23 J. Burés, *Angew. Chem., Int. Ed.*, 2016, **55**, 2028.
- 24 E. Brunner, *J. Chem. Eng. Data*, 1985, **30**, 269.
- 25 Fitting the data to a model based on [**1**]<sub>2</sub> gave non-linear plots (see ESI† for further details).
- 26 Assuming the same rate law applies. Supported by computational calculations.
- 27 T. M. Alligrant and J. C. Alvarez, *J. Phys. Chem. C*, 2011, **115**, 10797.
- 28 I. Kaljurand, A. Kütt, L. Sooväli, T. Rodima, V. Mäemets, I. Leito and I. A. Koppel, *J. Org. Chem.*, 2005, **70**, 1019.
- 29 T. A. Rokob, A. Hamza and I. Pápai, *J. Am. Chem. Soc.*, 2009, **131**, 10701.
- 30 Et<sub>3</sub>N and DMAP: Z. Glasovac, M. Eckert-Maksić and Z. B. Maksić, *New J. Chem.*, 2009, **33**, 588; PMP: M. Dworniczak and K. T. Leffek, *Can. J. Chem.*, 1990, **68**, 1657; DBU and TBTMG: C. F. Lemaire, J. J. Aerts,



L. C. Libert, F. Mercier, D. Goblet, A. R. Plenevaux and A. J. Luxen, *Angew. Chem., Int. Ed.*, 2010, **49**, 3161.

31 The energy values reported correspond to solution phase Gibbs free energies that are based on  $\omega$ B97X-D/Def2TZVPP electronic energies, and all additional terms obtained at

the  $\omega$ B97X-D/Def2SVP level. See ESI† for full computational details.

32 In FLPs with early TSs, such as  $\text{Mes}_3\text{P/B}(\text{C}_6\text{F}_5)_3$ , a KIE of only 1.1 has been obtained (see ref. 22).

